ELSEVIER

PII: S0144-8617(97)00012-X

Carbohydrate Polymers **32** (1997) 213–221
Published by Elsevier Science Ltd
Printed in Great Britain
0144-8617/97/$17.00 + .00

Screening the physical properties of novel *Pseudomonas* exopolysaccharides by HPSEC with multi-angle light scattering and viscosity detection[1]

Marshall L. Fishman,* Paola Cescutti,[†] William F. Fett, Stanley F. Osman, Peter D. Hoagland and Hoa K. Chau

Eastern Regional Research Center, Agricultural Research Service, U.S. Department of Agriculture, 600 East Mermaid Lane, Wyndmoor, PA 19038, USA

(Received 12 September 1996; revised version received 4 December 1996; accepted 6 December 1996)

The physical properties of three novel acidic exopolysaccharides obtained from *P. marginalis* types A, B and C, one from *P. 'gingeri'*, one from *P. andropogenis* and one from *P. fluorescens* have been partially characterized. These EPSs were chromatographed on three serially placed SE Shodex OH pak columns covering a molar mass range for pullulans from about 4×10^7 to 1×10^3. The mobile phase was 0.05 M $NaNO_3$. Physical measurements were performed on about 30 mg of sample for each EPS. The weight average molar mass of these EPSs ranged from about 0.71 to 2.85×10^6, the weight average intrinsic viscosity from 7.15 to 35.3 dl/g and the radius of gyration from 62 to 123 nm. The polydispersities of these EPSs ranged from 1.01 to 1.37. The large molar mass, size and viscosities of these EPSs may indicate that they have potential for use as thickeners, stabilizers, emulsifiers, and gelling agents in the food and non-food industries. Published by Elsevier Science Ltd

INTRODUCTION

Since the 1960s, when xanthan gum became commercially available, there has been a continuing search for other bacterial exopolysaccharides (EPSs) with physical properties that would allow them to be exploited as thickeners, stabilizers, emulsifiers and gelling agents in the food and nonfood industries. During the course of screening studies in our laboratory designed to identify bacteria which produce alginate, we discovered six novel acidic exopolysaccharides produced by members of the genus *Pseudomonas*. The structures of four of the EPSs have been elucidated (Fig. 1). The first acidic EPS identified was produced by *P. marginalis* strain HT041B, a plant pathogen, and was given the trivial name marginalan (Osman & Fett, 1989) (Fig. 1, *P. marginalis* type A). Production of this EPS was later found to occur in strains of the saprophytic bacteria *P. fluorescens* and *P. putida* (Fett *et al.*, 1989, 1995). Recently, the succinate substituent was reassigned to the galactose moiety of the repeating unit (Matulova *et al.*, 1996). Subsequently, two additional EPSs produced by other strains of *P. marginalis* were identified (Osman & Fett, 1990, 1993) and were named *P. marginalis* types B and C (Fig. 1). These three EPSs do not contain uronic acid but are acidic due to the presence of the non-sugar substituents succinate, pyruvate or lactic acid. The fourth EPS is produced by the mushroom (*Agricus bisporus*) pathogen *P. 'gingeri'* and does contain a uronic acid as well as pyruvate (Cescutti *et al.*, 1995) (Fig. 1). Most recently, two additional EPSs have been identified, but their complete structures have not yet been determined. The first is produced by the saprophytic bacterium *P. fluorescens* strain H13. The extracellular material obtained from this bacterium and used in this study was found to contain glucose, glucosamine, rhamnose, fucose, arabinose and acetate (Fett *et al.*, 1995). Very recent results indicate that the primary acidic EPS present in this material contains glucose, *N*-acetyl glucosamine and *N*-acetyl aminomannuronic acid

*To whom correspondence should be addressed.
[1]Mention of brand or firm names does not constitute an endorsement by the US Department of Agriculture over others of a similar nature not mentioned.
[†]Permanent address: Department of Biochemistry, Biophysics and Macromolecular Chemistry, University of Trieste, Italy.

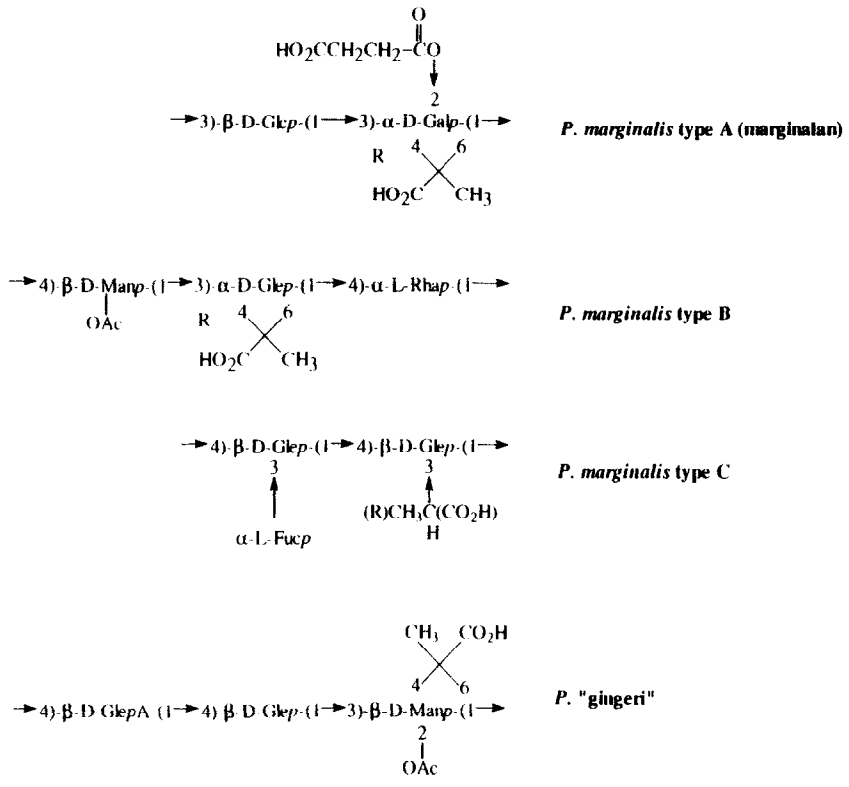

Fig. 1. Novel pseudomonad exopolysaccharides with elucidated structures. *P., Pseudomonas*; Glc, glucose; Gal, galactose; Man, mannose; OAc, -*O*-acetyl; Rha, rhamnose; Fuc, fucose; GlcpA, glucuronic acid in the pyranose form; R, absolute configuration of the asymmetric carbon.

(Osman, S. F., unpublished data). The sixth acidic EPS found is produced by the plant pathogen *P. andropogonis* and contains glucose, glucuronic acid, mannose, rhamnose and galactose (Osman, S. F. unpublished data).

In this study we have determined several physical properties (molar mass, radius of gyration, intrinsic viscosity and the concentration dependence of refractive index) of these polymers using small amounts of each sample (approximately 30 mg). This was possible by use of HPSEC with online refractive index, viscometric, and laser light scattering detection. It was not necessary to rely on column calibration with macromolecules to obtain molar mass or radius of gyration for the EPSs under investigation. Wyatt (1993) has described the theory and practice of online light scattering measurements whereas Haney (1985) has similarly described online viscometry so these will not be repeated here.

MATERIALS AND METHODS

Materials

Pullulan standards were obtained from JM Science Inc., Grand Island, NY, whereas dextran standards were obtained from Pharmacia LKB Biotechnology, Piscataway NJ and Sigma Chemical Co., St Louis, MO. Reagent grade $NaNO_3$ was obtained from Mallinckrodt-Baker, Phillipsburg, NJ. HPLC grade water was obtained by passing house deionized water through a Modulab Polisher I deionizer–filtration system (Continental Water Systems Corp., San Antonio, TX). All media components were obtained from Difco Laboratories, Detroit, MI, except for the protease Alcalase 2.4 L (Novo Nordisk Bioindustrials Inc., Danbury, CT).

Preparation of bacterial exopolysaccharides

Pseudomonas marginalis type A EPS (marginalan) was prepared from cultures of strain HT041B grown on *Pseudomonas* agar F (PAF) for 4 days at 20°C. *Pseudomonas marginalis* type B EPS was prepared from cultures of strain PF-05-2 grown on PAF for 3 days at 28°C and *P. marginalis* type C EPS from cultures of strain ATCC 10844 grown on PAF for 7 days at 20°C. EPS of *P. 'gingeri'* was prepared from cultures of strain Pf9 grown on PAF for 3 days at room temperature. The additional two EPSs were prepared from cultures grown in liquid media. Starter cultures of *P. fluorescens* strain H13 and *P. andropogenis* strain 27 were grown overnight in nutrient broth (8 g/l)–yeast extract (5 g/l) medium (NBY) and 10 ml was used to inoculate 500 ml of either modified King's medium B (King *et al.*, 1954) with Bacto tryptone substituted for proteose peptone #3 and containing increased levels of glycerol (50 g/l)

(strain H13) or nutrient broth (8 g/l)–yeast extract (5 g/l)–dextrose (50 g/l) with Alcalase 2.4 l at a final concentration of 0.005% (v/v) (strain 27) contained in 2800 ml Fernbach flasks. Cultures were incubated for 5 days at 20°C with shaking (250 rpm).

To isolate EPS, the mucoid growth on solid media was scraped off the media using distilled water and a bent glass rod and the suspension was stirred vigorously. Broth cultures and the suspensions obtained from solid media were subjected to centrifugation (16 300*g*, 30–60 min) and the clear supernatant fluids were collected. A concentrated aqueous solution of KCl (25%, w/v) was added to give a final concentration of 1% and then EPS was precipitated by addition of 2–3 volumes of cold (4°C) isopropanol. After sitting at 4°C for at least 2 h, the precipitated EPS was collected by centrifugation (16 300 *g*, 15 min) and the EPS-containing pellets re-dissolved in distilled water. Precipitation with isopropanol was repeated two more times as described above.

The samples were then subjected to dialysis against distilled water at 4°C. After dialysis, any insoluble material was removed by centrifugation (16 300 *g*, 30 min) and the supernatant fluids lyophilized. The lyophilized preparations were taken up in 50 mM Tris–HCl buffer, pH 7.5 with 10 mM $MgCl_2$ to give a final concentration of 1 mg EPS/ml. The EPS preparations were then subjected to digestion with DNase, RNase and protease (alcalase 2.4 L) (all used at 25 μg/ml), re-dialysis against distilled water, 0.5 M NaCl, distilled water and finally ultracentrifugation (100 000 *g*, 4 h) to remove any contaminating nucleic acid, protein and lipopolysaccharide. The supernatant fluids were lyophilized. The final EPS samples were taken up in distilled water and the resultant solutions showed no peak absorbance at 260 or 280 nm. In distilled water, the pH of all EPSs except *P. andropogenis* were 6.2–6.3. The pH of *P. andropogenis* EPS was 6.6. The pH values and method of preparation would indicate that the EPSs were substantially in the K^+ form (Danta *et al.*, 1994).

Sample preparation

EPS (10–20 mg) and 10 ml of 0.05 M $NaNO_3$ were placed in a covered beaker, stirred for 30 min and refrigerated overnight. Immediately prior to analysis by chromatography, each sample was stirred for 15 min and equilibrated at 45°C for 20 min.

Chromatography

Two separate chromatographs were used in these experiments, one for online light scattering measurements and the other for online viscometry measurements. All macromolecular solutions were passed through a 0.40 or 0.20 μm Nucleopore filter (Costar Corp, Cambridge, MA) prior to analysis. Sample injection volume was 100 μl. The mobile phase was 0.05 M $NaNO_3$ prepared with house-distilled water treated with a Modulab polisher, and filtered with a 0.4 μm Nucleopore membrane before degassing. The nominal flow rate was 0.7 ml/min. Columns were thermoregulated at 45°C in a water bath.

For light scattering measurements, the chromatography system consisted of a model KT-35 Shodex degasser (JM Science Inc., Grand Island, NY) connected in series to a model 6000A pump fitted with an M-45 pulse dampener (Waters Assoc., Milford, MA), in-line 0.1 μm vv Durapore membrane filter housed in a high pressure holder (Millipore Corp., Milford, MA), 15′ stainless steel warming coil, i.d. 0.04″, model 210 injection valve (Beckman, Palo Alto, CA), 10×3.2 mm i.d. Synchropak cartridge guard column (SynChrom, Inc, Lafayette, IN), three chromatography columns, Dawn F MALLS photometer fitted with a Helium–Neon laser ($\lambda = 632.8$ nm) and a K-5 flow cell (Wyatt Tech., Santa Barbara, CA), and a model SE-61 Shodex differential refractive index detector (DRI) (JM Science Inc.). The serially placed chromatography columns were Shodex OH-pak SB-806, SB-805, and SB-803 (JM Science Inc.). The exclusion limits for these columns as specified by the manufacturer for pullulans are 4×10^7, 2×10^6, 1×10^5 g/mol, respectively. Each column is 8 mm i.d. ×300 mm length.

The electronic outputs of the DRI and the MALLS were sent to a 486 PC. The data were processed with ASTRA™ (v. 2.11) and EASI™ (v. 6.0) (Wyatt Tech). The DRI response factor was measured by injecting a series of known NaCl concentrations directly into the detector cell with a syringe. This response factor was obtained from the slope of the linear plot between NaCl concentration and RI response. The factor to correct the Rayleigh ratio at 90° (R_{90}) for instrument geometry was obtained by measuring the scattering intensity of toluene at 90° and tested with pullulan standards. The responses to scattered light intensity of the photodiodes arrayed around the scattering cell at angles other than 90° were normalized to the diode at 90° with a P-50 pullulan standard. The scattering angles in degrees available for intensity measurements were 22.26, 29.11, 36.46, 44.72, 54.19, 65.02, 77.11, 90.00, 102.89, 114.98, 125.81, 135.28, 143.54, 150.89, and 157.74. As suggested by Jeng & Balke (1993) molar masses and radii were extracted from data fit to Debye equations. Data for PA EPS were fitted by linear least squares to a 2nd order Debye equation whereas all the other EPSs were fitted to a 3rd order Debye equation. Debye equations were fitted iteratively, deleting those detected angles whose standard deviation from the least squares fit was greater than twice the average standard deviation of all detectors fitted. In most cases data from the detector at 22.26° were deleted. In a few cases data from the detector at 29.11° and/or at 154.74° were deleted.

For viscosity measurements, Four Synchropak GPC columns (2×GPC4000, 1×GPC1000, 1×GPC100,

SynChrom, Inc., Lafayette, IN) were connected in series. The fractionating range of these columns was about the same as the Shodex OH pak columns. Each column was 4.5 mm i.d. ×250 mm length. An on-line Degasser ERC-3120 (Erma Optical Works, Ltd., Tokyo) was connected to a Beckman Model 110 pump with a Model 421 controller. The pump output was sent to a Beckman pulse filter and two Waters M45 pulse dampeners. Samples were introduced with a Beckman Model 210 injector valve. Concentration was measured by differential refractive index with a model 405 Viscotek laser refractometer ($\lambda = 670$ nm), Viscotek Corp., Houston, TX, and viscosity by a model 100 Viscotek differential viscometer. The RI detector was calibrated with vacuum dried dextran standards. The viscometer was checked with pullulan standards to insure that accurate intrinsic viscosities were measured. The electronic output of the refractometer and the viscometer were sent to a 486 PC. The data were processed with Viscotek, TriSec GPC software.

Determination of change in refractive index with concentration (d*n*/d*c*)

Dextran (T-110) was dried overnight under vacuum. The polysaccharide was introduced manually by means of a syringe connected to the inlet valve of the Viscotek laser refractometer. Triplicate plateau heights were obtained. The following equation was used to determine the unknown d*n*/d*c*:

$$[dn/dc]_u = [dn/dc]_k[(ht)_u(c)_k]/[(ht)_k(c)_u] \quad (1)$$

where $[dn/dc]_u$ is the d*n*/d*c* of the unknown exopolysaccharide; $[dn/dc]_k$ is the d*n*/d*c* of Dextran T110; $(ht)_u$ = plateau height of the unknown; $(c)_k$ = concentration of Dextran T110; $(ht)_k$ = plateau height of Dextran T110; $(c)_u$ = concentration of unknown.

RESULTS

Table 1 contains d*n*/d*c* values for the various exopolysaccharides (EPS)s. Because monosaccharide composition of the trisaccharide repeating unit differs only by one residue and both contain pyruvate substituents (Fig. 1), the d*n*/d*c* value for *P. 'gingeri'* EPS (PGI) (see Fig. 1) was assumed to be identical with the EPS from *P. marginalis* type B (PMB).

The superimposed refractive index (RI) and 90° light scattering intensity (LS) chromatograms for *P. andropogenis* are shown in Fig. 2a, (PA) EPS. The RI chromatogram indicates a monomodal polysaccharide distribution with small amounts of two low molecular weight impurities, whereas the LS chromatogram indicates a bimodal distribution with a trace concentration of microgel. These occur in spite of extensive dialysis, ultracentrifugation and ultrafiltration. Molar masses

Table 1. Concentration dependence of refractive index (d*n*/d*c*)[a] of bacterial EPSs

Exopolysaccharide	d*n*/d*c*
PA	0.168(0.001)[b]
PMB	0.174[c]
PGI	0.174(0.001)
PMC	0.172(0.007)
PMA	0.151(0.003)
PFL	0.157(0.002)

[a]Units: ml/g.
[b]Standard deviation of triplicate determinations.
[c]Value not determined. Used same value as determined for *P. 'gingeri'*.
PA, *P. andropogenis*; PMB, *P. marginalis*, type B; PGI *P. 'gingeri'*; PMC *P. marginalis*, type C; PMA, *P. marginalis*, type A; PFL, *P. fluorescens*.

computed from integration over the entire chromatogram (Table 2) with the aid of a 2nd order Debye equation gave a M_w of about 720 000 and polydispersities of 1.43 and 1.77 for M_w/M_n and M_z/M_n, respectively. As typified by the data in Fig. 2b measured at the 90° light scattering peak maximum, a 2nd order Debye plot was required to fit the angular dependence of the excess scattered light. In Fig. 2c the superimposed plots of molar mass against volume for two replicates are shown. About 10% of the chromatogram area, mostly at the low molar mass end of the chromatogram, contains highly scattered points. The software enables the lower end of the chromatogram to be linearly extrapolated as shown by the straight line at the low molar mass end of the plot in Fig. 2c. The extrapolated data for PA in Table 3 reveals that M_w decreases slightly (to about 0.71×10^6) as compared to the value computed from the non-extrapolated chromatogram due to somewhat more scattered points above the extrapolated line than below it. Extrapolation reduces M_w/M_n to 1.37 indicating a marginally more narrow polysaccharide distribution after extrapolation than before. Because M_z remains about the same and M_n decreases after extrapolation, the value of M_z/M_n increases to about 1.88. A more rapid initial rise of the LS as compared to the RI chromatogram in addition to an appreciably lower value of M_w/M_n as compared to M_z/M_n is consistent with the interpretation that there is a small amount of microgel in the preparation.

In Fig. 3a are shown the superimposed RI and 90° LS chromatograms for the EPS from PMB. As typified by the data in Fig. 3b measured at the 90°light scattering peak maximum, a 3rd order Debye plot was required to fit the angular dependence of the excess scattered light. This was true for all EPSs except PA. The molar masses before and after extrapolation are contained in Table 2. Comparison of molar mass averages in Table 2 for PMB EPS reveals that there is only a slight change in M_n and M_w before and after extrapolation whereas M_z decreases by one-third of its original value. The decrease

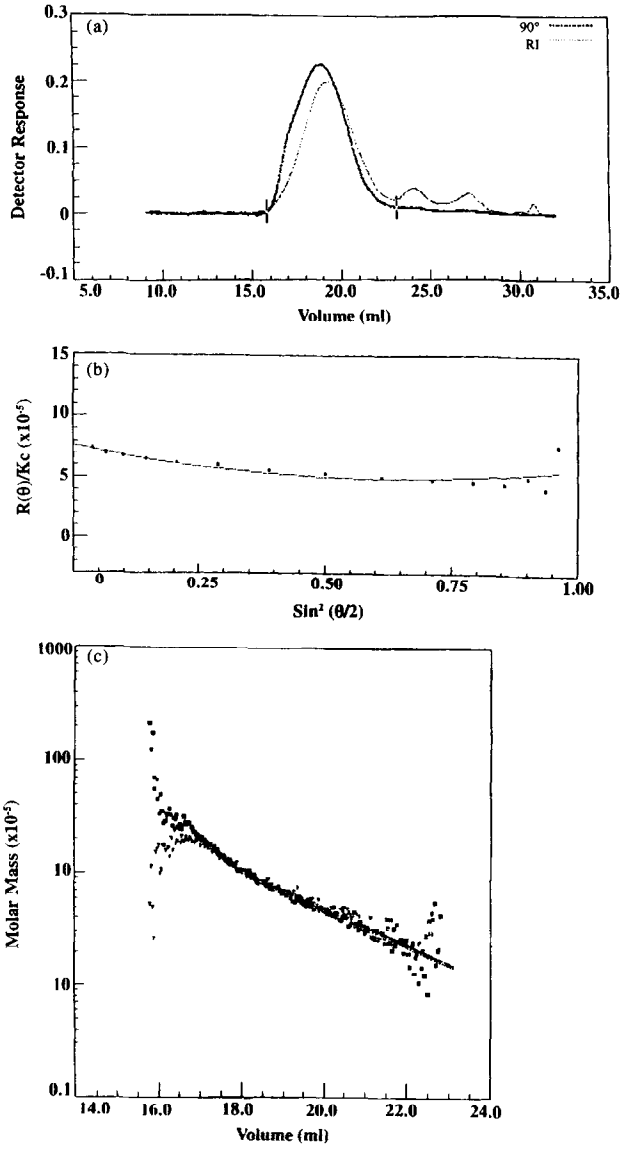

Fig. 2. (a) Superimposed 90° light scattering and refractive index (RI) chromatograms of exopolysaccharide from *P. andropogenis*. Injected concentration 2 mg/ml, mobile phase 0.05 M $NaNO_3$, injected volume 100 µl, flow rate 0.7 ml/min. (b) Second order Debye plot at peak maximum for exopolysaccharide from *P. andropogenis*. Triangular point indicates angle rejected because standard deviation from the least squares fit was greater than twice the average standard deviation of all detectors fitted. (c) Dependence of molar mass on elution volume for exopolysaccharide from *P. andropogenis*. Straight line is extrapolation of data at low end of chromatogram in (a).

in the value of M_z after extrapolation probably indicates that extrapolation removes an excess of scattered points with erroneously high molar mass values. These points occur at the low molecular weight end of the chromatogram where LS signal to noise is poor. As shown by the data in Table 2, PMB EPS is almost monodispersed with a molar mass of about 1×10^6.

In Fig. 4a are shown the superimposed RI and angular LS chromatograms for the EPS from *P. 'gingeri'* (PGI). As shown by the data in Table 2, PGI EPS also was almost monodispersed and had a molar mass of about 1×10^6. Chromatograms obtained for *P. marginalis* type C (PMC) EPS and *P. marginalis* type A (PMA) EPS were similar in shape to that obtained for PGI EPS (data not shown). The data in Table 2 reveals that the EPS from PMC had the least polydispersity of any of the EPSs measured and a molar mass of *ca* 1.5×10^6. PMA EPS had a molar mass of about 1.7×10^6 and had a M_w/M_n value of 1.14 and an M_z/M_n value of 1.29.

In Fig. 5 are shown the superimposed RI and 90° LS chromatograms for the EPSs from *P. fluorescens* (PFL). In this case two macromolecular components were resolved partially. The higher molar mass component accounted for about 89% of the sample by weight as measured by RI. As shown by the data in Table 2, the major component had a molar mass of about 2.85×10^6 and was almost monodispersed. By partial integration of the 2nd half of the chromatogram, we estimated that the minor compositional component had a molar mass of about 2.2×10^6 and had a M_w/M_n value of 1.05 and an M_z/M_n value of 1.1. Table 2 also contains molar mass data for EPSs from three bacteria, PMB, PMI, and PMC, each measured at injected concentrations of 1 mg/ml. PMB and PGI EPSs showed an increase in molar mass of about 20% and an increased polydispersity. PMC EPSs showed a slight decrease in molar mass and a slight increase in polydispersity. These changes may reflect increases in LS signal to noise ratio as a result of lower sample concentrations.

Table 3 contains the number(R_{gn}), weight(R_{gw}) and Z-(R_{gz}) average root mean square radii of gyration for these bacterial EPSs. A plot of radius against elution volume before and after extrapolation for superimposed replicate samples is shown for PGI in Fig. 4b. In this case there was no significant difference between the extrapolated and non-extrapolated data. Consistent with molar mass data, the extrapolated data in Table 3 shows that PA is the EPS which is most polydispersed in size as indicated by differences in radii moment averages. Table 3 also contains radii for EPSs from three bacteria, PMB, PMI, and PMC, each measured at injected concentrations of 1 mg/ml. In this case, the three EPSs showed little or no change in size when compared to radii measured at 2 mg/ml.

Table 4 contains number (IV_n), weight (IV_w) and Z-(IV_z) average intrinsic viscosities (IV) measured at injected concentrations of 2 mg/ml. As revealed by values of IV_w/IV_n and IV_z/IV_n , three EPSs were somewhat more polydisperse than the rest. For these three EPSs, the order of polydispersity was PA > PMA > PFL.

The EPS from PFL had a much larger polydispersity as measured by viscosity than measured by light scattering because the minor macromolecular component was not included in the light scattering calculation. Table 4 also contains IVs for PMB, PGI, and PMC

Table 2. Molar masses ($\times 10^{-6}$) of bacterial EPSs

Exopolysaccharide	M_n	M_w	M_z	M_w/M_n	M_z/M_n
PA[a]	0.55(0.01)[d]	0.72(0.01)	0.97(0.02)	1.43	1.77
PMB[a]	0.98(0.01)	1.05(0.03)	1.63(0.08)	1.07	1.66
PGI[a]	1.12(0.04)	1.15(0.04)	1.45(0.05)	1.04	1.27
PMC[a]	1.53(0.02)	1.62(0.02)	2.12(0.2)	1.06	1.39
PMA[a]	1.72(0.09)	1.84(0.1)	2.03(0.2)	1.08	1.18
PFL[a]	2.95(0.07)	3.03(0.1)	3.76(0.1)	1.03	1.28
PA[b]	0.52(0.01)	0.71(0.01)	0.98(0.02)	1.37	1.88
PMB[b]	0.97(0.03)	1.02(0.03)	1.05(0.03)	1.05	1.09
PGI[b]	0.98(0.03)	1.06(0.04)	1.15(0.07)	1.08	1.17
PMC[b]	1.48(0.02)	1.49(0.03)	1.50(0.3)	1.01	1.02
PMA[b]	1.47(0.01)	1.68(0.03)	1.90(0.2)	1.14	1.29
PFL[b]	2.81(0.2)	2.85(0.2)	2.87(0.2)	1.01	1.02
PMB[c]	1.07(0.09)	1.20(0.06)	1.59(0.2)	1.13	1.41
PGI[c]	1.10(0.02)	1.25(0.06)	1.50(0.1)	1.14	1.36
PMC[c]	1.36(0.02)	1.40(0.2)	1.43(0.2)	1.07	1.06

[a]Integration of entire refractive index chromatogram. Injected concentration 2 mg/ml.
[b] Extrapolation of linear data. Injected concentration 2 mg/ml.
[c] Extrapolation of linear data. Injected concentration 1 mg/ml.
[d] Standard deviation of triplicate determinations. Debye 2nd order equation used for PA. For all other samples a 3rd order Debye equation was used.
PA, *P. andropogenis*; PMB, *P. marginalis*, type B; PGI *P. 'gingeri'*; PMC *P. marginalis*, type C; PMA, *P. marginalis*, type A; PFL, *P. fluorescens*.

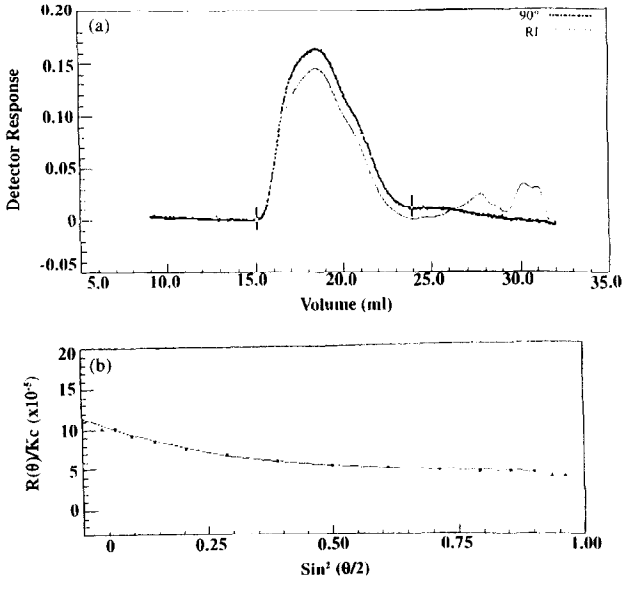

Fig. 3. (a) Superimposed 90° light scattering and refractive index (RI) chromatograms of *P. marginalis* type B exopolysaccharide. Injected concentration 2 mg/ml, mobile phase 0.05 M $NaNO_3$, injected volume 100 μl, flow rate 0.7 ml/min. (b) Third order Debye plot at peak maximum for *P. marginalis* type B exopolysaccharide. Triangular point indicates angle rejected because standard deviation from the least squares fit was greater than twice the average standard deviation of all detectors fitted.

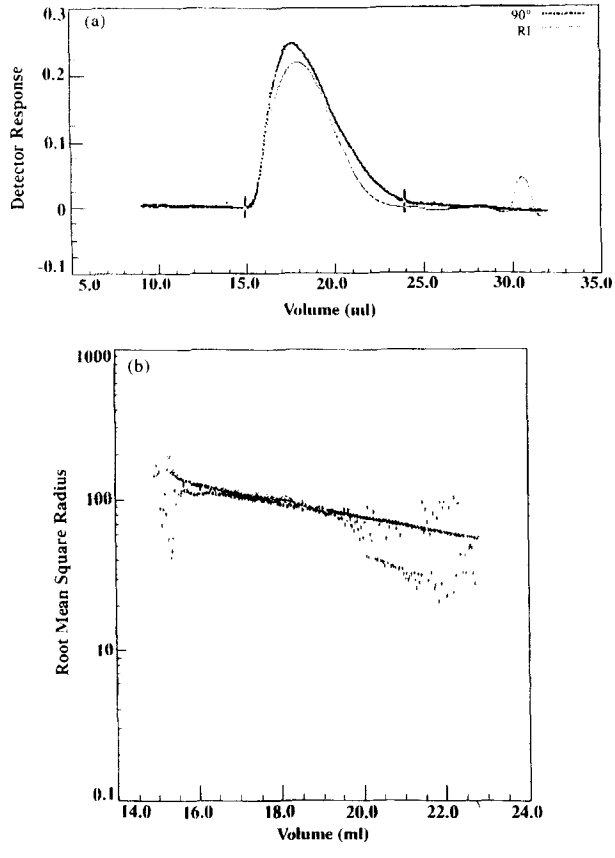

Fig. 4. (a) Superimposed 90° light scattering and refractive index (RI) chromatograms of *P. 'gingeri'* exopolysaccharide. Injected concentration 2 mg/ml, mobile phase 0.05 M $NaNO_3$, injected volume 100 μl, flow rate 0.7 ml/min. (b) Dependence of root mean square radius of gyration (nm) on elution volume for *P. 'gingeri'* exopolysaccharide. Straight line is extrapolation of scattered data at low end of chromatogram in (a).

EPSs measured at injected concentrations of 1 mg/ml. The IV values for PMB EPS were not significantly different at the two injected concentrations whereas the value for PMC EPS was somewhat higher and the value for PGI EPS somewhat lower at 1 mg/ml than at 2 mg/ml injected concentration. No trend was observed in *IV*

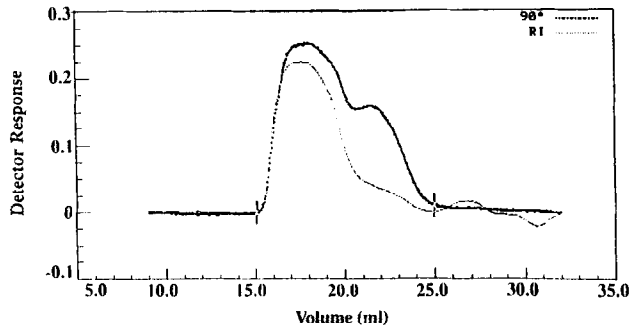

Fig. 5. Superimposed 90° light scattering and refractive index (RI) chromatograms of *P. fluorescens* exopolysaccharide. Injected concentration 2 mg/ml, mobile phase 0.05 M $NaNO_3$, injected volume 100 μl, flow rate 0.7 ml/min.

with injected concentration. These differences are probably related to the difficulty in handling highly viscous samples.

Table 3. Root mean square radii of gyration (nm) of bacterial EPSs

Exopolysaccharide	R_{gn}	R_{gw}	R_{gz}
PA[a]	50(8)[c]	56(6)	62(3)
PMB[a]	93(6)	95(6)	97(7)
PGI[a]	101(5)	105(6)	108(6)
PMC[a]	111(3)	112(3)	112(3)
PMA[a]	101(5)	105(6)	108(6)
PFL[a]	122(6)	123(5)	123(5)
PMB[b]	98(1)	102(1)	106(3)
PGI[b]	102(5)	106(5)	110(5)
PMC[b]	100(7)	102(5)	104(4)

[a] Extrapolation of linear data. Injected concentration 2 mg/ml.
[b] Extrapolation of linear data. Injected concentration 1 mg/ml.
[c] Standard deviation of triplicate determinations. Debye 2nd order equation used for PA. For all other EPSs a 3rd order Debye equation was used.
PA, *P. andropogenis*; PMB, *P. marginalis*, type B; PGI *P. 'gingeri'*; PMC *P. marginalis*, type C; PMA, *P. marginalis*, type A; PFL, *P. fluorescens*.

DISCUSSION

Although the EPSs examined in this study differ in their primary structure (Fig. 1), we wanted to estimate whether their solution properties are comparable. One way to conduct this investigation with the data provided by this screening process is to look at some variables as a function of molar mass. Normally this process is most appropriately employed with linear macromolecules which are structurally identical but only differ in molecular weight. Nonetheless, we have applied these techniques to the EPSs examined, keeping in mind their structural differences.

In Fig. 6, we have plotted R_{gz} values against M_w values for each EPS on a double logarithmic scale. A correlation coefficient of about 0.81 was found between R_{gz} and M_w. Even this degree of correlation between these two parameters seems rather surprising given the differences in sugar residues and their sequences in the backbone, backbone linkages, substituents, and attachments of substituents relative to one another for the EPSs characterized. The relationship between R_{gz} and M_w was found to be $R_{gz} \sim M_w^{0.41}$. The value of 0.41 for the scaling law exponent indicates a rather slow increase in size with molar mass. In the case of a series of structurally identical polymers differing only in size and molar mass, the low exponent could be attributed to a series of compact spherical coils differing only in size. Because of the structural differences cited above and the limited molar mass range of the EPSs it is unlikely that the numerical value of the exponent can be used to determine the shape of these EPSs. When PA EPS is not included in the plot, the correlation coefficient increases to 0.87 and the exponential decreases to 0.18. This relatively high linear correlation between R_{gz} and M_w may indicate some similarity in shape for all the EPSs with PA EPS being the most dissimilar in shape.

In Fig. 7 is plotted R_{gz}^2/M_w against $M_w^{0.5}$. The term,

Table 4. Intrinsic viscosities (dl/g) of bacterial EPSs

Exopolysaccharides	IV_n	IV_w	IV_z	IV_w/IV_n	IV_z/IV_n
PA[a]	4.1(0.1)[c]	7.1(0.1)	9.5(0.3)	1.7	2.3
PMB[a]	34.3(1)	35.3(1)	36.5(1.6)	1.03	1.06
PGI[a]	30.0	30.6	31.4	1.02	1.05
PMC[a]	25.2(1)	25.5(1)	25.9(1)	1.01	1.02
PMA[a]	6.6(0.5)	8.1(0.1)	10.7(1)	1.22	1.62
PFL	11.0(0.5)	12.6(0.3)	13.6(0.2)	1.14	1.23
PMB[b]	33.0(1)	36.9(3)	39.5(3)	1.11	1.20
PGI[b]	23.8(3)	25.4(3)	26.5(2)	1.07	1.11
PMC[b]	29.9(1)	29.9(1)	29.9(1)	1.00	1.00

[a] Extrapolation of linear data. Injected concentration 2 mg/ml.
[b] Extrapolation of linear data. Injected concentration 1 mg/ml.
[c] Standard deviation of triplicate determinations. Debye 2nd order equation used for PA. For all other EPSs a 3rd order Debye equation was used.
PA, *P. andropogenis*; PMB, *P. marginalis*, type B; PGI *P. 'gingeri'*; PMC *P. marginalis*, type C; PMA, *P. marginalis*, type A; PFL, *P. fluorescens*.

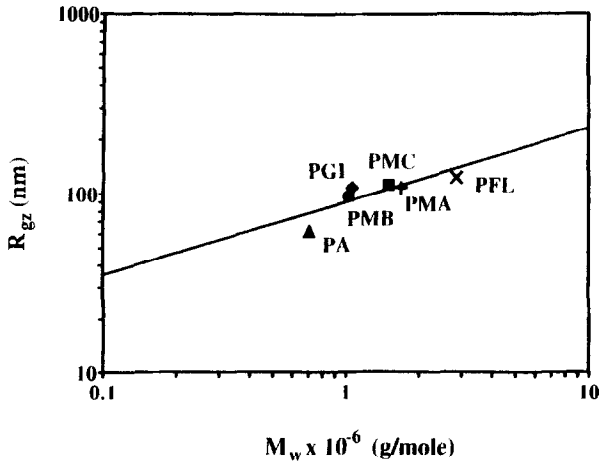

Fig. 6. Dependence of *z*-average root mean square radius of gyration on molar mass for pseudomonad exopolysaccharide. PA, *P. andropogenis*; PGI, *P. 'gingeri'*; PMB, *P. marginalis* type B, PMC *P. marginalis* type C; PMA, *P. marginalis* type A; PFL, *P. fluorescens*.

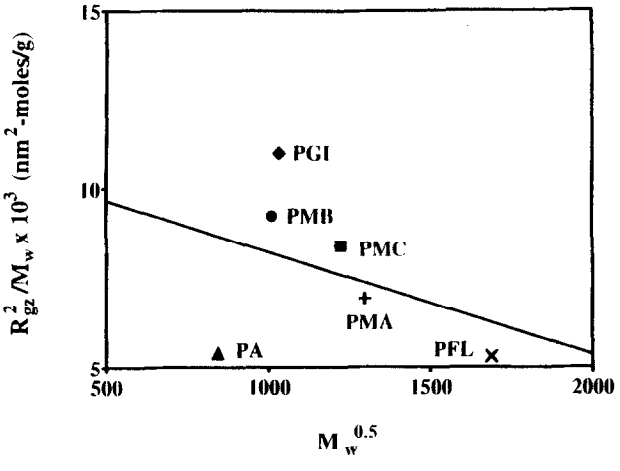

Fig. 7. Dependence of normalized cross sectional area (NCSA) on molar mass for pseudomonad exopolysaccharides. PA, *P. andropogenis*; PGI, *P. 'gingeri'*; PMB, *P. marginalis* type B, PMC *P. marginalis* type C; PMA, *P. marginalis* type A; PFL, *P. fluorescens*.

R_g^2 is the cross-sectional area through the center of a sphere generated by the Brownian motion of a molecule, with root mean square radius R_g and normalized by its molar mass. This plot has been used to measure changes in chain expansion for a series of amyloses which only differ in molar mass and to compare intrinsic extensions of these molecules in different solvents (Roger & Colonna, 1992). Recently, the normalized cross sectional area (NCSA) has been used to distinguish between amylose and amylopectin in corn starches which were analyzed by HPSEC with online viscosity and refractive index detection (Fishman & Hoagland, 1994). In this case, it was shown that differences in chain branching on relatively narrow fractions eluting from the column set were responsible for their differences in NCSA. The data in Fig. 7 is more difficult to interpret than the two cases mentioned previously because of structural differences among the EPS but some information can be ascertained from the plot. The linear correlation coefficient was 0.37 but when PA EPS is excluded from the plot, the correlation coefficient becomes 0.92. This high correlation between NCSA and M_w for five of the six EPSs may indicate that there is a similarity in the solution conformation among the five EPSs in spite of structural differences. It is interesting to note that there is a decrease in NCSA (i.e. more compact chain packing) with increasing molar mass for these five EPSs. Chain compaction with molar mass on somewhat similar macromolecules might occur if intramolecular attractive forces were greater than excluded volume effects between polymer segments. On the other hand, chain folding or intermolecular aggregation could also explain a decrease in NCSA with molar mass.

By way of comparison, recent work on native xanthan revealed it had a molar mass of about 9×10^6 and an *IV* of 56 dl/g, whereas a sample degraded by sonication had a molar mass of 1.2×10^6, an *IV* of about 12.4 dl/g and a R_g of about 95 nm (Milas *et al.*, 1996). In that work and another recent report (Chazeau *et al.*, 1995), it was suggested that the shape of xanthan could be described by the worm-like chain model. Thus, EPSs from PMB, PGI, PMC, and PFL all have molar masses, *IV*s, and R_gs comparable to, or somewhat larger than, xanthan with a molar mass of about 1.2×10^6. Possibly, these EPSs have extended chain structures comparable to xanthan. PMA may also be an extended chain in solution because of its reasonably high NCSA value. In contrast, PA has a smaller M_w, IV_w and larger R_{gz} and polydispersity than the other EPSs.

CONCLUSIONS

Analysis indicated that the preparation containing PMC EPS was monodisperse and microgel free, well within experimental error. Preparations of EPS from PMB, PGI and PMA were of relatively narrow distribution. The EPS preparation from PFL contained a major and a minor component. The major EPS (≈89%) was monodispersed and microgel free. The EPS from PA had the lowest molar mass and was the most polydisperse of the EPSs studied. Thus, PA is most likely to differ from the other EPSs in its chain extension in solution.

EPSs from PMB, PGI, PMC and PFL have *IV*s, R_gs, and molar masses comparable to or greater than sonicated native xanthan with an M_w of about 1.2 million but significantly lower than unsonicated native xanthan. EPS from PMA has an *IV* somewhat lower than the sonicated xanthan mentioned but a higher R_g and M_w. Based on the comparisons with sonicated xanthan and with each other it is expected that EPSs from PMB, PGI, PMC, PMA and PFL, like sonicated xanthan,

have extended worm-like chain configurations in solutions. Furthermore, the relatively large molar mass, size and viscosities of these EPSs indicate that they may have potential for use as thickeners, stabilizers, emulsifiers and gelling agents in the food and nonfood industries.

REFERENCES

Chazeau, L., Milas, M. and Rinaudo, M. (1995) Conformations of xanthan in solution: Analysis by steric exclusion chromatography. *International Journal of Polymer Analysis and Characterization* **2,** 21–29.

Cescutti, P., Osman, S. F., Fett, W. F. and Weisleder, D. (1995) The structure of the acidic exopolysaccharide produced by *Pseudomonas 'gingeri'* strain Pf9. *Carbohydrate Research* **275,** 371–379.

Dantas, L., Heyraud, A., Courtois, B., Courtois, J. and Milas, M. (1994) Physicochemical properties of 'Exogel' exocellular β (1-4)-D-glucuronan from *Rhizobium meliloti* strain M5N1 C.S. (NCIB 40472). *Carbohydrate Polymers* **24,** 185–191.

Fett, W. F., Osman, S. F. and Dunn, M. F. (1989) Characterization of exopolysaccharides produced by plant-associated fluorescent pseudomonads. *Applied Environmental Microbiology* **55,** 579–583.

Fett, W. F., Wells, J. M., Cescutti, P. and Wijey, C. (1995) Identification of exopolysaccharides produced by fluorescent pseudomonads associated with commercial mushroom (*Agaricus bisporus*) production. *Applied Environmental Microbiology* **61,** 513–517.

Fishman, M. L. and Hoagland, P. D. (1994) Characterization of starches dissolved in water by microwave heating in a high pressure vessel. *Carbohydrate Polymers* **23,** 175–183.

Jeng, L. and Balke, S. T. (1993) Evaluation of light scattering detectors for size exclusion chromatography. II. Light scattering equation selection *Journal of Applied Polymer Science* **49,** 1375–1385.

Haney, M. A. (1985) The differential viscometer, II. Online viscosity detector for size exclusion chromatography. *Journal of Applied Polymer Science* **30,** 3037–3049.

Matulov'a, M., Navarini, L., Osman, S. F. and Fett, W. F. (1996) NMR analysis of galactoglucan from *Pseudomonas marginalis*: assignment of the ^{1}H and ^{13}C NMR spectra and location of succinate groups. *Carbohydrate Research* **283,** 195–205.

Milas, M., Reed, W. F. and Printz, S. (1996) Conformations and flexibility of native and renatured xanthan in aqueous solutions. *International Journal of Biological Macromolecules* **18,** 211–221.

Osman, S. F. and Fett, W. F. (1989) Structure of an acidic exopolysaccharide of *Pseudomonas marginalis* HT041B. *Journal of Bacteriology* **171,** 1760–1762.

Osman, S. F. and Fett, W. F. (1990) The structure of the acidic exopolysaccharide of *Pseudomonas marginalis* strains PF-05-2 and PM-LB-1. *Carbohydrate Research* **199,** 77–82.

Osman, S. F. and Fett, W. F. (1993) Structure of the acidic exopolysaccharide of *Pseudomonas marginalis* strain ATCC 10844. *Carbohydrate Research* **242,** 271–275.

Roger, P. and Colonna, P. (1992) The influence of chain length on the hydrodynamic behavior of amylose. *Carbohydrate Research* **227,** 73–83.

Wyatt, P. J. (1993) Light scattering and the absolute characterization of macromolecules. *Analytica Chimica Acta* **272,** 1–40.